CHEMICAL ENGINEERING TRANSACTIONS

VOL. 70, 2018

A publication of AIDIC
The Italian Association of Chemical Engineering
Online at www.aidic.it/cet

Guest Editors: Timothy G. Walmsley, Petar S. Varbanov, Rongxin Su, Jiří J. Klemeš
Copyright © 2018, AIDIC Servizi S.r.l.
ISBN 978-88-95608-67-9; **ISSN** 2283-9216

DOI: 10.3303/CET1870124

Numerical Investigation of a Packed-Bed Active Magnetic Regenerator

Haoning Shi, Ting Ma, Qiuwang Wang*

Key Laboratory of Thermo-Fluid Science and Engineering, Ministry of Education, Xi'an Jiaotong University, Xi'an, Shaanxi 710049, China
wangqw@mail.xjtu.edu.cn

Magnetic refrigeration at room temperature is of great potential for the new generation of refrigeration technology. The performance of the active magnetic regenerator is greatly influenced by many design and operation parameters. In this paper, a one-dimensional numerical model for active magnetic regenerator is presented and validated. The performances of active magnetic regenerator with different particle diameters, utilization factors and operating frequencies are calculated with the present model. The performance curves of utilization factor with different particle diameters are presented and analysed. The results indicate that the cooling power and COP both increase at first and then decrease with the increase of the utilization factor. And the deviation between the optimal utilization factor of cooling power and COP becomes larger with decrease of the particle diameter. Comprehensively, the optimal range of particle diameter is 0.4-0.6 mm with the utilization factor of 0.7-1.5 which also depends on the operating frequency based on the present data.

1. Introduction

Magnetic refrigeration at room temperature is an emerging and promising refrigeration technology based on the magnetocaloric effect (MCE). The MCE is the thermal response of magnetocaloric material (MCM) in the process of magnetization or demagnetization. In the application of magnetic refrigeration, the use of traditional refrigerants CFC and HCFC can be completely avoided, which means no damage to the ozone layer and no contribution to the greenhouse effect. The compressor is not required as well thus leading to a compact structure without much noise. Therefore, the magnetic refrigeration is of great potential for the replacement of the vapor compression refrigerator technology. In recent decades, a great number of studies on magnetic refrigeration at room temperature have been performed. In summary, the researches mainly focus on two aspects, i.e., the magnetic prototypes and the numerical models. Recently, a number of prototypes have been created. Jacobs et al. (2014) presented and tested a large-scale rotary magnetic refrigerator. Its cooling power achieved 2502 W over a temperature span of 11 K, with electrical COP of 1.9. Trevizoli et al. (2016) designed and built a single packed-bed active magnetic regenerator (AMR) with 195.5 g of Gd spheres. The performance of the AMR under different operating frequencies and utilization factors has been evaluated. Its COP achieved 4.6 with a temperature span of 5 K, at 0.25 Hz working frequency. Eriksen et al. (2015) built a rotary active magnetic regenerator (AMR) prototype. Its cooling power achieved 103 W and the COP was 3.1 under a temperature span of 10.2 K. Meanwhile, a number of numerical studies have been performed. Nielsen et al. (2011) reviewed the published models of AMR. Tušek et al. (2011) presented a one-dimensional model for the operation of AMR. The model has been used to analyse cases under different operating conditions. Lionte et al. (2015) numerically analysed a reciprocating AMR by a two-dimensional mathematical model. The regenerator performance was evaluated and the detailed data of the temperature and velocity fields in the microchannel was presented. Based on the previous studies, it has been widely accepted that the AMR performance and the heat transfer characteristics are closely related, and the heat transfer characteristics are directly affected by the particle diameter. However, the utilization factor should also be considered when optimizing the particle diameter. The interaction effect among the particle diameter, utilization factor and operating frequency should be discussed. In this work, a one-dimensional numerical

Please cite this article as: Shi H., Ma T., Wang Q., 2018, Numerical investigation of a packed-bed active magnetic regenerator , Chemical Engineering Transactions, 70, 739-744 DOI:10.3303/CET1870124

model for AMR is presented and validated. The performances of AMR with different particle diameters, utilization factors and operating frequencies are calculated and analysed.

2. Mathematic model

Viewed from the heat transfer process, the magnetic refrigeration system consists of a cold heat exchanger (CHEX), an active magnetic regenerator (AMR) and a hot heat exchanger (HHEX). As shown in Figure 1, the CHEX and HHEX are connected with the cold end and the hot end of AMR respectively. The AMR is the heat transfer channel of packed bed structure. It is made of the magnetocaloric material. In this work, gadolinium(Gd) is selected as the magnetocaloric material.

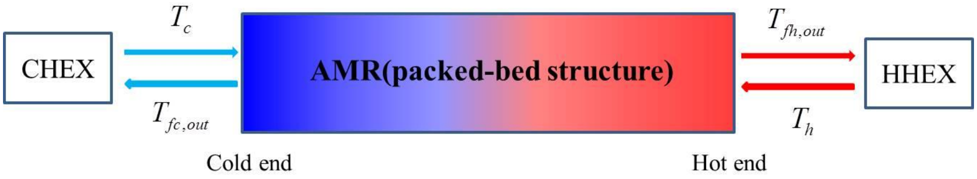

Figure 1: Basic components of heat transfer system of magnetic refrigerator

Based on the MCE, periodic change of the AMR's temperature field is achieved by periodic magnetization and demagnetization process. The heat or cold quantity generated in the AMR is carried away by the periodic oscillating heat transfer fluid to the HHEX and CHEX. Finally, the heat transfer between the fluid and the cold source or the heat source occurs in the CHEX and the HHEX. Specifically, each complete AMR cycle consists of four stages successively:

1) Magnetization: No fluid flows, the magnetic field is increased, and the magnetocaloric packed bed heats up due to MCE.

2) Cold flow: Fluid flows from the cold end to the hot end, absorbs heat from the packed bed, and then releases heat to the hot source in the HHEX.

3) Demagnetization: No fluid flows, the magnetic field is reduced, the magnetocaloric packed bed cools down due to MCE.

4) Hot flow: Fluid flows from the hot end to the cold end, releases heat to the packed bed, and then absorbs heat from the cold source in the CHEX, which provides the cooling power.

After a certain number of such magnetocaloric cycles, the temperature gradient along the length direction of AMR will be established and the temperature profile of the AMR will achieve a periodic steady state. For simplification, several important assumptions are made as follows:

1) In the process of magnetization, the applied magnetic field is uniform.

2) There is no heat loss to/from the surroundings in the AMR, the adiabatic boundary condition is adopted at both the cold end and hot end of the AMR.

3) The fluid velocity of cold and hot flow is regarded as constant and the fluid flow is uniform.

4) The fluid thermal properties are regarded as constants.

5) The heat transfer process in cold or hot heat exchanger is considered sufficient enough that the fluid can be heated or cooled to the cold or hot source temperature.

6) The magnetization and demagnetization are both linear process, and the time ratio of the 4 stages is kept as 1:4:1:4 (From magnetization to hot flow).

The governing equations for energy of fluid and solid domains can be expressed as follows:

$$\frac{\partial T_f}{\partial t}+u\frac{\partial T_f}{\partial x}=\frac{\lambda_{f,eff}}{\rho_f c_f \varepsilon}\frac{\partial^2 T_s}{\partial x^2}+\frac{h_{eff}A_{ht}}{\rho_f c_f V\varepsilon}(T_s-T_f)+\frac{u}{\rho_f c_f}\frac{dp}{dx} \tag{1}$$

$$\frac{\partial T_s}{\partial t}=\frac{\lambda_{s,eff}}{\rho_s c_s(1-\varepsilon)}\frac{\partial^2 T_s}{\partial x^2}+\frac{h_{eff}A_{ht}}{m_s c_s}(T_f-T_s)-\frac{T_s}{c_s}\frac{\partial M}{\partial T_s}\frac{\partial \mu_0 H}{\partial t} \tag{2}$$

T_s, T_f, u, ε, h_{eff}, A_{ht}, M, H represent the solid temperature, the fluid temperature, the fluid velocity, the porosity, the effective convective heat transfer coefficient, the heat exchange area, the magnetization intensity, the magnetic field intensity. The first term and the second term on the right side of Eqs(1, 2) are the thermal conductivity term and the convection heat transfer term. The third term on the right side of Eq(1) is the viscous loss source term of fluid flow, which reflects the fluid friction loss in the packed-bed structure due to fluid viscosity. The viscous loss is greatly related to the fluid velocity and the pressure drop. The magnetocaloric source term is coupled into the governing equation of solid domain, which is effective at the stage of magnetization or demagnetization. The use of the magnetocaloric source term requires the support of detailed data of the magnetization intensity and the specific heat capacity of magnetocaloric material under different temperatures and magnetic fields. In this work, the related data of Gd are calculated using the Mean field model (Tishin A.M. et al., 2003). The magnetic intensity and specific heat capacity of Gd as functions of temperature are shown in Figures 2a and b.

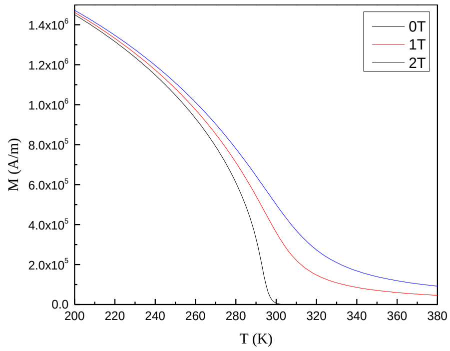

(a)

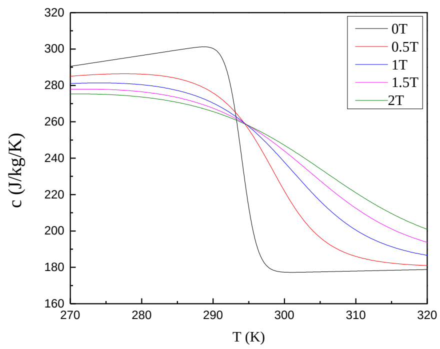

(b)

Figure 2: The magnetocaloric properties of Gd as a function of temperature under different magnetic fields(a) The magnetic intensity; (b) The specific heat capacity

The effective thermal conductivity for solid and fluid can be expressed as follows (Wakao et al., 1982):

$$\lambda_{f,eff} = \varepsilon\lambda_f + 0.5\,\mathrm{Pr}\,\mathrm{Re}\,\lambda_f \tag{3}$$

$$\lambda_{s,eff} = (1-\varepsilon)\lambda_s \tag{4}$$

The pressure gradient can be calculated by the correlation as follow, which is given by Kaviany (1995):

$$\frac{dp}{dx} = \frac{90}{\mathrm{Re}}\frac{1-\varepsilon}{\varepsilon^2} + 0.9\frac{1-\varepsilon}{\varepsilon^3} \tag{5}$$

The Nusselt number is calculated by the correlation for a spherical packed-bed structure given by Wakao et al. (1982):

$$Nu = 2 + 1.1\mathrm{Re}^{0.6}\,\mathrm{Pr}^{1/3} \tag{6}$$

A correction factor related to the packed-bed structure is applied to balance the temperature distribution perpendicular to the fluid flow in solid domain as follow (Kitanovski et al., 2015):

$$h_{eff} = \frac{h}{1+\frac{Bi}{3}} \tag{7}$$

h is the convective heat transfer coefficient and Bi is the Biot number. The adiabatic boundary conditions are adopted at both the cold end and hot end of the AMR, and the temperature of fluid that enters the AMR is considered as the temperature of cold source or hot source.
At cold flow stage (Fluid flows from the cold end to the hot end):

$$T_{f,x=0} = T_c, \left.\frac{\partial T_f}{\partial x}\right|_{x=L} = 0, \left.\frac{\partial T_s}{\partial x}\right|_{x=0} = 0, \left.\frac{\partial T_s}{\partial x}\right|_{x=L} = 0 \tag{8}$$

At hot flow stage (Fluid flows from the hot end to the cold end):

$$T_{f,x=L} = T_h, \left.\frac{\partial T_f}{\partial x}\right|_{x=0} = 0, \left.\frac{\partial T_s}{\partial x}\right|_{x=0} = 0, \left.\frac{\partial T_s}{\partial x}\right|_{x=L} = 0 \tag{9}$$

As shown in Figure 3, the computational domain consists of the fluid domain and the solid domain. The finite volume method is used for the numerical discretization. The computation is completed with the MATLAB software. The unsteady state calculation is carried out with the implicit scheme. The numerical calculation will continue for a certain number of cycles until the periodic steady operating state is reached. The key performance parameters of the AMR can be obtained when the steady state is reached, specifically including the heating power, cooling power, and COP.
In the cold flow stage, the heating power transferring to the hot source in the HHEX can be expressed as:

$$Q_h = \int_{\tau_m}^{\tau_m+\tau_f} \dot{m}_f c_f (T_{fh,out} - T_h) dt / 2(\tau_m + \tau_f) \tag{10}$$

In the hot flow stage, the cooling power transferring to the cold source in the CHEX can be expressed as:

$$Q_c = \int_{2\tau_m+\tau_f}^{2(\tau_m+\tau_f)} \dot{m}_f c_f (T_c - T_{fc,out}) dt / 2(\tau_m + \tau_f) \tag{11}$$

τ_m and τ_f are the time of magnetization (demagnetization) and hot (cold) flow in one cycle respectively. COP is the ratio of the cooling power and the input work, which can be expressed as:

$$COP = \frac{Q_c}{Q_h - Q_c} \tag{12}$$

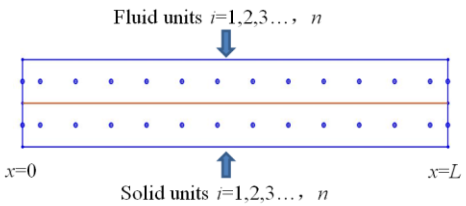

Figure 3: Schematic of the discretization of AMR

3. Results and discussion

3.1 Validation of present model

The present numerical model is validated by solving the temperature field of a single-blow transient passive regenerator. As shown in Figure 4, the result of the temperature profile is in accordance with the simplified Schumann solution (Shitzer et al., 1983) and Engelbrecht's results (Engelbrecht et al., 2008) under the same operating condition. The validity of the numerical model for unsteady calculation has been proved.

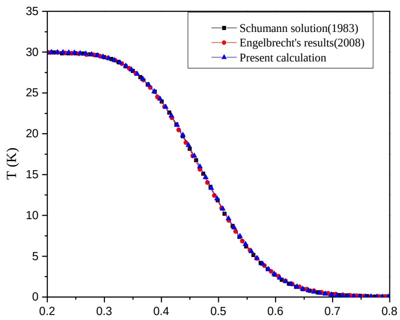

Figure 4: Comparison of the regenerator temperature predicted by the simplified Schumann solution (1983), Engelbrecht (2008) and present results

3.2 Influence of operating frequency, utilization factor, and particle diameter on AMR performance

By numerical calculation with the present model, the performance of the AMR under different operating frequencies, utilization factors, and particle diameters is obtained. In the calculation, the geometric and operating parameters of AMR are listed in Table 1. Utilization factor (UF), a non-dimensional parameter of mass flow rate, is defined as below:

$$UF = \frac{\dot{m}_f c_f \tau_f}{m_s \overline{c_s}} \tag{13}$$

$\dot{m}_f$ is the fluid mass flow rate, m_s is the total mass of the magnetocaloric material, $\overline{c_s}$ is the average specific heat of the magnetocaloric material.

Table 1: Constant geometric and operating parameters of AMR

Constant geometric and operating parameters of AMR	
Dimensions of the AMR	120 mm (length)×40 mm×20 mm
Heat-transfer fluid	Water
Porosity	0.4
Operating frequency	1 Hz/2 Hz
Utilization factor	0-3
Particle diameter	0.2/0.4/0.6/0.8/1.0 mm
Magnetic field change	0—1 T
Temperature span	12 K (T_c =288 K, T_h=300 K)

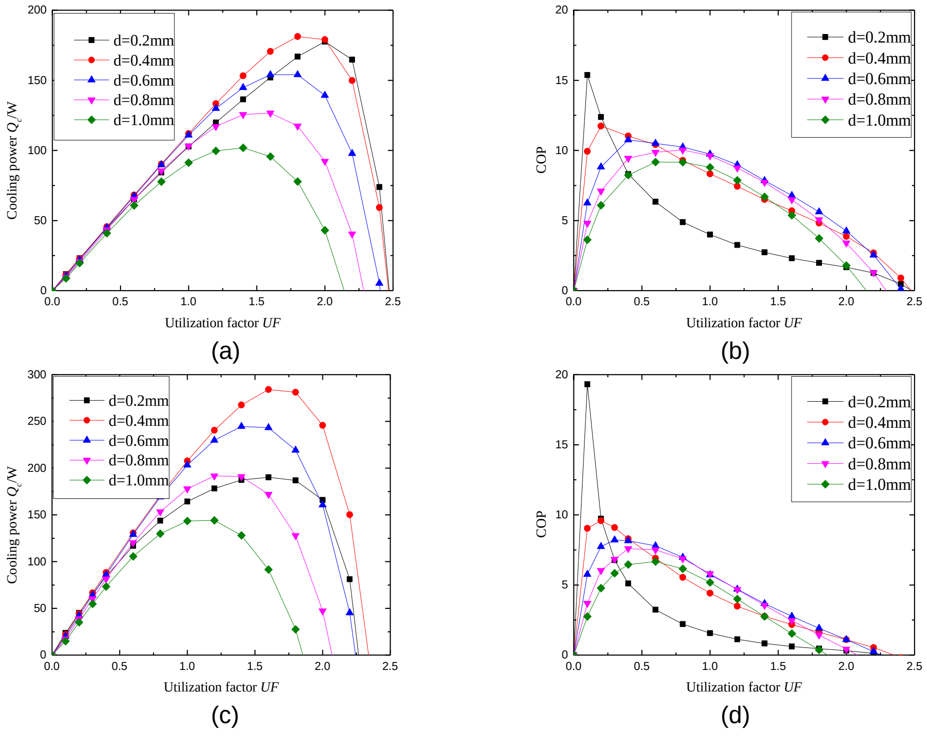

Figure 5: Cooling power and COP as functions of UF for different particle diameters (a) cooling power of 1 Hz; (b) COP of 1 Hz; (c) cooling power of 2 Hz; (d) COP of 2 Hz

As shown in Figure 5, with increase of the UF, the cooling power and COP both increase at first and then decrease under different particle diameters and frequencies. Generally, with increase of the UF, the COP reaches its maximum earlier than the cooling power. Such results are in good agreement with the previous study (Tušek et al.,2011). Specifically, with decrease of the particle diameter, the deviation between the optimal UF of cooling power and COP becomes larger, which is not desirable. Besides, as the particle diameter is reduced from 1.0 mm to 0.4 mm, the maximal cooling power increases gradually. Generally, with the decrease of the particle diameter, the heat transfer in AMR is more sufficient, thus increasing the refrigeration capacity of AMR. However, the maximal cooling power of d=0.4 mm is greater than d=0.2 mm, shown in Figures 5(a) and (c). This trend becomes more obvious when the operating frequency is 2 Hz in comparison with 1 Hz. Such result can be explained by the viscous loss source term in the energy equation. The viscous heating effect has negative effect on the refrigeration capacity, which cannot be ignored for the packed-bed AMRs. Especially, the influence of viscous losses is much more significant when the size of magnetocaloric particle is small. Comprehensively, the optimal range of particle diameter is 0.4-0.6 mm with the utilization factor of 0.7-1.5 in consideration of both cooling power and COP, which also depends on the operating frequency. Finally, as the operating frequency increases from 1 Hz to 2 Hz, the cooling power increases, however, the overall level of COP decreases as the expense.

4. Conclusions

In this study, a 1-D numerical model for AMR is presented and validated. By numerical calculation with the present model, the performances of the AMR under different operating frequencies, utilization factors, and particle diameters are obtained. Based on the present study, several conclusions are obtained as follows:

1) With increase of the UF, the cooling power and COP both increase at first and then decrease under different particle diameters and frequencies.

2) With decrease of the particle diameter, the deviation between the optimal UF of cooling power and COP becomes larger, which is not desirable.

3) In this work, the optimal range of particle diameter is 0.4-0.6 mm, with the utilization factor of 0.7 - 1.5 which also depends on the operating frequency. A comprehensive optimization combing the numerical model and the optimization algorithm is needed for the accurate optimal operation based on this work.

Acknowledgments

This work is financially supported by the International Cooperation and Exchanges Project of NSFC of China (Grant No. 51120165002), National Natural Science Foundation of China (Grant No. 51306139) and the Fundamental Research Funds for the Central Universities.

References

Engelbrecht K., 2008, A numerical model of an active magnetic regenerator refrigerator with experimental validation, Ph.D. Thesis, University of Wisconsin-Madison, Madison, USA.

Eriksen D., Engelbrecht K., Bahl C.R.H., Bjørk R., Nielsen K.K., Insinga A.R., Pryds N., 2015, Design and experimental tests of a rotary active magnetic regenerator prototype, International Journal of Refrigeration, 58, 14-21.

Jacobs S., Auringer J., Boeder A., Chell J., Komorowski L., Leonard J., Russek S., Zimma C., 2014, The performance of a large-scale rotary magnetic refrigerator, International Journal of Refrigeration, 37, 84-91.

Kaviany M., 1995, Principles of heat transfer in porous media, 2nd Edition. Springer, Berlin, Germany.

Kitanovski A., Tušek J., Tomc U., Plaznik U., Ožbolt M., Poredoš A., 2015, Magnetocaloric energy conversion, Springer International Publishing, Zurich, Switzerland.

Lionte S., Vasile C., Siroux M., 2015, Numerical analysis of a reciprocating active magnetic regenerator, Applied Thermal Engineering, 75, 871-879.

Nielsen K.K., Tusek J., Engelbrecht K., Schopfer S.,Kitanovski A., Bahl C.R.H., Smith A., Pryds N., Poredos A., 2011, Review on numerical modeling of active magnetic regenerators for room temperature applications, International Journal of Refrigeration , 34(3), 603-616.

Shitzer A., Levy M., 1983, Transient behavior of a rock-bed thermal storage system subjected to variable inlet air temperatures: analysis and experimentation, Journal of Solar Energy Engineering, 105, 200-206.

Tishin A.M., Spichkin Y.I., 2003, The magnetocaloric effect and its applications, Institute of Physics Publishing Bristol, UK, and Philadelphia, USA.

Trevizoli, P.V., Nakashima, A.T., Peixer, G.F., Barbosa, J.R., 2016, Performance evaluation of an active magnetic regenerator for cooling applications – part I: Experimental analysis and thermodynamic performance, International Journal of Refrigeration, 72, 192-205.

Tušek J., Kitanovski A., Prebil I., Poredoš A., 2011, Dynamic operation of an active magnetic regenerator (AMR): numerical optimization of a packed-bed AMR, International Journal of Refrigeration, 34(6), 1507-1517.

Wakao, N., Kagei, S., 1982, Heat and mass transfer in packed beds, Taylor & Francis, New York, USA.